DOI: 10.1007/s12541-012-0238-5

Preparation of Doped $BaZrO_3$ and $BaCeO_3$ from Nanopowders

Rojana Pornprasertsuk[1,2,#], **Chonhathai Yuwapattanawong**[1], **Sirorat Permkittikul**[1], and **Thanawan Tungtidtham**[1]

1 Research Unit of Advanced Ceramics, Department of Materials Science, Faculty of Science, Chulalongkorn University, Bangkok, Thailand, 10330
2 Center of Excellence on Petrochemical and Materials Technology, Chulalongkorn University, Bangkok, Thailand, 10330
Corresponding Author / E-mail: rojana.p@chula.ac.th, TEL: +66-2-218-5547, FAX: +66-2-218-5561

KEYWORDS: Barium cerate, Barium zirconate, Calcination, Nanopowder, Processing, Sintering

---

To lower the calcining and sintering temperatures of 16 at% Y-doped $BaZrO_3$ (BYZ), Gd-doped $BaCeO_3$ (BGC) and Sm-doped $BaCeO_3$ (BSC), nanopowders of $BaCO_3$ and either (i) yttria stabilized zirconia, (ii) Gd_2O_3 and CeO_2 or (iii) Sm_2O_3 and CeO_2, were used as starting materials, respectively. BYZ powders were prepared by two mixing methods (i.e. ball milling and magnetic stirring), followed by calcination at 1050-1250 °C, while BSC and BGC powders were prepared by ball milling and calcined at 1050 °C. The results reveal that the ball milling and magnetic stirring methods yield similar results for BYZ powder preparation. By adding 1 wt% ZnO nanopowder, the average relative densities of BYZ pellets were increased from ~70% to ~96% at the sintering temperatures of 1300 °C. Thus, with the utilization of nanopowders and ZnO as a sintering aid, the calcining and sintering temperatures were lowered to 1050 °C and 1300 °C, respectively, while still attaining the relative bulk densities of both BYZ and BGC higher than 95.7%. However, since the relative bulk density of BSC reached only 93% even sintered at 1400 °C, ZnO was not an effective sintering aid for the BSC fabrication.

Manuscript received: December 8, 2011 / Accepted: May 15, 2012

1. Introduction

Doped $BaZrO_3$ and $BaCeO_3$ have been extensively studied as electrolyte materials for protonic ceramic fuel cell (PCFC) applications. Y-doped $BaZrO_3$ (BYZ), Gd-doped $BaCeO_3$ (BGC) and Sm-doped $BaCeO_3$ (BSC) were focused in this study, due to their high proton conductivities over the PCFC operating temperature range.[1-11] The major drawback for the utilization of these materials is their high sintering temperatures of above 1600 °C for doped $BaZrO_3$[1-6] and above 1450 °C for doped $BaCeO_3$[7-12] to achieve the relative densities of > 93% required for fuel cell applications.

Several studies have pursued to lower the sintering temperatures of these materials.[9,12-17] Babilo and Haile[15] and Gorbova et al.[9] studied the effect of NiO, CuO and ZnO as sintering aids on BYZ and BGC. Gorbova et al.[9] achieved the relative density of 97, 92 and 94% with the addition of NiO, ZnO and CuO, respectively, in 10 at% BGC pellets (calcined at 1150 °C and sintered at 1450 °C). Babilo and Haile[15] prepared the BYZ powder by a glycine-nitrate combustion synthesis process and reported the relative density of BYZ pellet (4 mol% ZnO addition) at 95% after sintered at 1300 °C. Due to the presence of $Ba_2YCu_3O_x$ phase in Cu-modified BYZ and the change of color in Ni-modified BYZ pellets, ZnO became the most suitable sintering aid for BYZ.[15] Tao and Irvine[13,14] and Peng et al.[16] also observed the increase in the sinterability of BYZ pellets with 1 wt% ZnO addition prepared by the conventional method (calcined at > 1400 °C and sintered at > 1325 °C). Tao and Irvine[14] achieved the relative densities of 96% for $BaZr_{0.8}Y_{0.2}O_{3-\delta}$ (1 wt% ZnO) and 97% for $BaCe_{0.5}Zr_{0.3}Y_{0.16}Zn_{0.04}O_{3-\delta}$ at the sintering temperature of 1325 °C.

Our previous work in Ref. 17 presented the fabrication of 6-40 at% BYZ pellets (1 wt% ZnO addition) using $BaCO_3$, 3 mol% yttria stabilized zirconia (YSZ) and two types of Y_2O_3: nano-sized and micro-sized powders. The results showed that the use of micro-Y_2O_3 caused the incomplete solid state reaction in 10-40 at% BYZ pellets calcined and sintered at 1400 °C, while the use of nano-Y_2O_3 BYZ pellets showed only a single perovskite phase. The larger grain size was also observed in nano-Y_2O_3 BYZ compared to micro-Y_2O_3 BYZ. Therefore, in this study, we have further increased the sinterability and lowered the calcining temperature by employing nanopowders for all starting materials of BYZ, BGC and BSC samples.

15-20 at% BYZ,[1,2,5,6,17,18] 15-20 at% BSC[10,11] and 15-25 at% BGC[7,8,12] were reported as the optimum doping concentration ranges for high proton conductivities. Therefore, in this study, we fabricated 16 at% BYZ, BGC and BSC pellets by the conventional method using $BaCO_3$, 8mol% YSZ, CeO_2, Sm_2O_3 and Gd_2O_3 nanopowders as starting materials and ZnO nanopowder as a sintering aid. Furthermore, to reduce the loss of nanopowder in ball milling process, the magnetic stirring technique was explored as an alternative method for the nanopowder mixing process. Effects of the mixing method (i.e. ball milling and magnetic stirring) and the addition of ZnO on the sintering temperature, microstructures, relative bulk densities and phases of the 16 at% BYZ, BGC and BSC pellets were subsequently investigated and analyzed.

2. Experimental Procedures

2.1 Preparation of $BaY_{0.16}Zr_{0.84}O_{3-\delta}$ from nanopowders

16 at% BYZ powder was prepared from nanopowders of 8 mol% YSZ (< 40 nm, MTI Cor.) and $BaCO_3$ (< 50 nm, MTI Cor.). Two methods of mixing were employed: (i) ball milling (24 h) and (ii) magnetic stirring (24 h) followed by an ultrasonic treatment (10 min). The ball-milling process using 3 mol% YSZ balls (ϕ = 3 mm) was carried out in isopropanol media, while the magnetic stirring was performed in either isopropanol or a mixture of diethlene glycol butyl ether (butyl carbitol) and ethanol (1:1 by volume) (BE) media. The latter solvent mixture was chosen according to the work by Somroop et al.,[19] which showed the stable suspension of $BaCO_3$ and YSZ nanopowders in this solvent mixture even without stirring for 24 h. The starting nanopowders were mixed, dried and calcined at 1050, 1150 and 1250 °C for 10 h. Since isopropanol and butyl carbitol had different boiling points (82 and 230 °C), the drying temperatures were set to 110 and 250 °C, respectively. 1 wt% ZnO nanopowder was then added to the calcined BYZ powder and mixed by the same mixing methods for 30 min. The BYZ pellets (ϕ = 13 mm) with and without 1 wt% ZnO addition were formed by uniaxial pressing of 0.5 g BYZ powders at 20 MPa followed by cold isostatic pressing at 220 MPa and sintered at 1300-1400 °C for 10 h for the relative bulk density, microstructure and phase stability comparison.

2.2 Preparation of $BaSm_{0.16}Ce_{0.84}O_{3-\delta}$ and $BaGd_{0.16}Ce_{0.84}O_{3-\delta}$ from nanopowders

BSC and BGC powders were prepared by ball milling the nanopowders of CeO_2 (< 50 nm, MTI Cor.), $BaCO_3$ (< 50 nm, MTI Cor.) and either Sm_2O_3 (40 nm, MTI Cor.) or Gd_2O_3 (< 80 nm, MTI Cor.), respectively, at the required stoichiometry in isopropanol media using 3 mol% YSZ balls (ϕ = 3 mm) for 24 h. The mixed powders were dried at 110 °C and calcined at 1050 °C for 10 h. Since the suspensions of starting powders were not stable in both isopropanol and BE media, we did not employ the magnetic stirring technique in BSC and BGC sample preparations. 1 wt% ZnO was added into the calcined powders and ball milled in isopropanol media for 30 min. The BSC and BGC pellets (ϕ = 13 mm) were formed by the same method as BYZ pellets and sintered at 1300-1400 °C.

2.3 Relative density, phase and microstructure analysis

The relative bulk densities (ρ_{bulk}) compared to the theoretical density of all BYZ, BSC and BGC pellets were obtained using Archimedes' method and averaged over 4-6 samples. The suspended weight in water of each pellet (W_{sus}) was measured using 4-digit digital scale (Sartorius, model BP 221S). The wet and dry weights (W_{wet} and W_{dry}, respectively) of the pellet were subsequently measured in air before and after drying at 105 °C for 24 h. The pellet bulk density was then calculated by Eq. 1, where ρ_{H_2O} =0.997 g/cm^3 at 25 °C.

$$\rho_{bulk} = \frac{W_{dry}}{W_{wet} - W_{sus}} \times \rho_{H_2O} \quad (1)$$

Phase and microstructure analyses were performed by X-ray diffraction (XRD; Bruker AXS diffractrometer employing Cu Kα radiation (λ = 0.154 nm) and operating at 40 kV and 60 mA) and scanning electron microscopy (SEM; JEOL model JSM 6480LV operating at 20 kV) techniques.

3. BYZ: Results and Discussion

3.1 Phase of BYZ powders and pellets

XRD results of BYZ powders after calcined at 1050-1250 °C for 10 h are shown in Figs. 1 and 2. Both ball milling and magnetic stirring techniques reveal the similar $BaZrO_3$ perovskite phase at

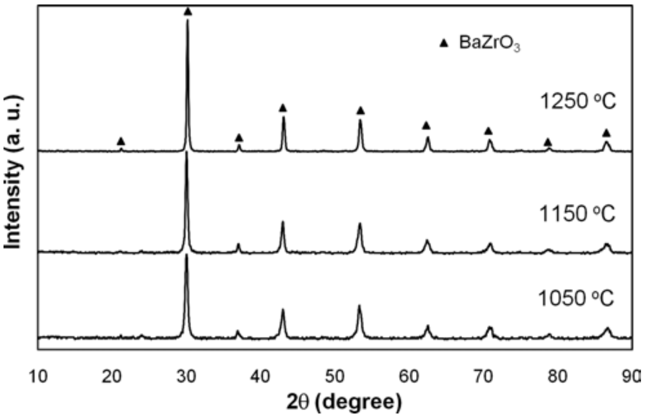

Fig. 1 XRD spectra of BYZ powders mixed by ball milling in isopropanol media and calcined at 1050-1250 °C for 10 h

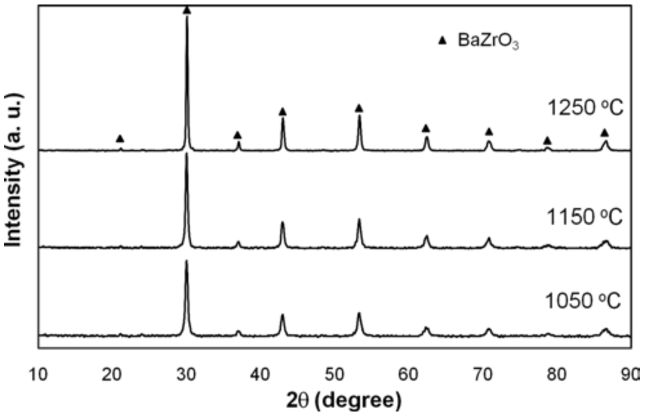

Fig. 2 XRD spectra of BYZ powders mixed by magnetic stirring in a BE media and calcined at 1050-1250 °C for 10 h

1050-1250 °C, thus suggesting that the calcined BYZ powder can also be prepared by the magnetic stirring technique. The magnetic stirring technique can substantially reduce the loss of mixed powders attached to YSZ balls in the ball milling process. The calcining temperature of 1050 °C achieved in this study is lower than those previously reported works,[4-6,14,16,17] which may arise from the enhancement of solid state reaction by high surface area of the nanopowders. The BYZ powder calcined at 1050 °C is subsequently chosen for BYZ pellet preparation.

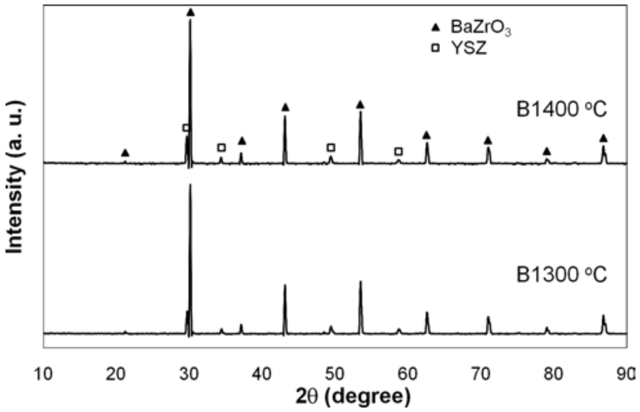

Fig. 3 XRD spectra of BYZ pellets prepared by ball milling (B), calcining at 1050 °C and sintering at 1300-1400 °C for 10 h

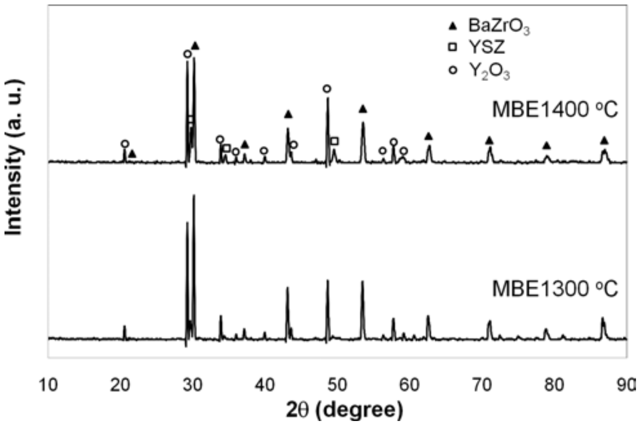

Fig. 4 XRD spectra of BYZ pellets prepared by magnetic stirring in a BE media (MBE), calcining at 1050 °C and sintering at 1300-1400 °C for 10 h

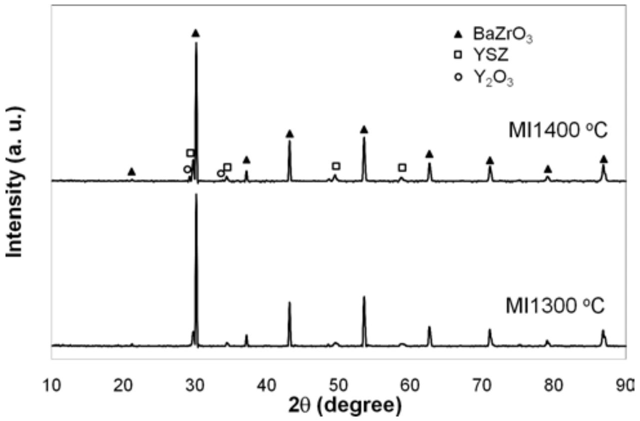

Fig. 5 XRD spectra of BYZ pellets prepared by magnetic stirring in isopropanol media (MI), calcining at 1050 °C and sintering at 1300-1400 °C for 10 h

XRD results of BYZ pellets after sintered at 1300-1400 °C are shown in Figs. 3-5. In Fig. 3, the XRD patterns of BYZ pellets prepared by ball-milling (referred to as B1300 and B1400) show the perovskite phase of $BaZrO_3$ (JCPDS: 06-0399) and slight amount of YSZ. Since YSZ phase is not observed in the calcined BYZ powder, it likely arises from the BaO loss on the surface of BYZ pellets during the sintering process as previously observed in Ref. 6, 18, 20.

However, the XRD results of BYZ pellets prepared by magnetic stirring in BE media sintered at 1300-1400 °C (referred to as MBE1300 and MBE1400, respectively) shows incredibly high fraction of Y_2O_3 phase (Fig. 4), which may arise from non-uniform dispersion of ZnO in the solvent and agglomeration of the calcined powders leading to poor sinterability and higher BaO loss.[14] The difference in the boiling points of butyl carbitol and ethanol in the BE media could affect the powder dispersibility due to the change of the solvent composition during drying. At the drying temperature of 250 °C, ethanol has a higher evaporation rate than butyl carbitol, which in turn causes the lower dispersibility and increasing agglomeration of the BYZ and ZnO powders upon drying.

Nevertheless, once the BE media was replaced by isopropanol (the same media used in the ball milling technique), XRD results of the BYZ pellets (Fig. 5), referred to as MI1300 and MI1400, became similar to those of B1300 and B1400 with additional trace of Y_2O_3 phase. Thus, the selection of solvent and drying temperature could affect the phase stability of the samples and became a crucial step for the magnetic stirring technique.

3.2 Relative bulk density and microstructure of BYZ pellets

According to our previous work,[17] the BaO-loss region was observed only in a range of hundred nanometers to a few microns from the BYZ surface. Thus, we neglect the effect of BaO evaporation in the theoretical bulk density calculation. Without ZnO additive, the pellets prepared by ball milling technique shows slightly higher relative bulk density (69.7-70.3%) compared to those mixed by magnetic stirring (66.6-67.3%) method. By adding 1 wt% ZnO nanopowder, the relative bulk density of BYZ pellets increases from ~70% to ~96%. Furthermore, the ZnO addition can enlarge the average grain size of BYZ from ~0.7 μm (Fig. 6(a)) to ~1.4 μm (Fig. 6(b)) due to the better sinterability of the pellets, in a

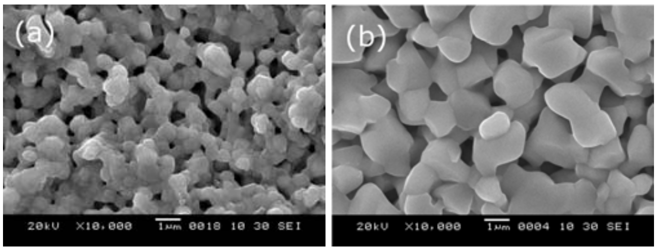

Fig. 6 SEM images of surfaces of BYZ pellets prepared by magnetic stirring in BE media, calcined at 1050 °C and sintered at 1400 °C for 10 h (a) without and (b) with 1 wt% ZnO addition

good agreement with Babilo and Haile[15] and Pornprasertsuk et al.[17] The increase in average grain size can eventually lower the overall grain boundary resistance of the BYZ sample.

The surfaces of all unpolished BYZ pellets become porous (Fig. 7(a) and 7(c)) due to the loss of BaO after sintering.[6,17,18,20] The surface porosity of unpolished BYZ pellets is increasing with increasing sintering temperature (Fig. 7(a) and 7(c)), in the same tendency as the increasing fraction of second phases in the XRD results (Fig. 3-5). However, the overall relative density of B1400 is still slightly higher than that of B1300. After the surface removal, dense surfaces are obtained as shown in Fig. 7(b) and 7(d), thus suggesting that Ba deficiency only occurs on the BYZ surfaces.

According to Fig. 8, the relative densities of all BYZ samples with 1 wt% ZnO addition are higher than 95.9%. The ball milling method provides slightly higher relative bulk density compare to the magnetic stirring. No significant difference in the relative bulk density is found between MI and MBE sintered at 1300-1400 °C. The highest relative density of the BYZ pellet in this study is achieved by (i) mixing nanopowders by the ball milling method, (ii) calcining at 1050 °C and (iii) sintering at 1400 °C with 1 wt% ZnO sintering aid.

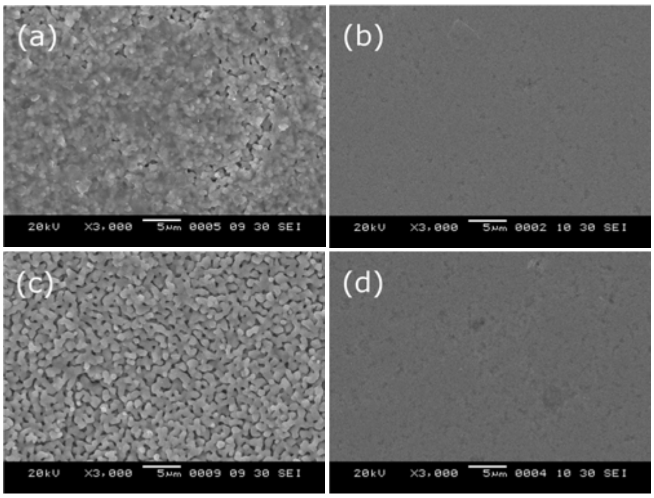

Fig. 7 SEM images of BYZ (1 wt% ZnO addition) surfaces prepared by ball milling and calcining at 1050 °C (a) unpolished sample sintered at 1300 °C (b) polished sample sintered at 1300 °C (c) unpolished sample sintered at 1400 °C and (d) polished sample sintered at 1400 °C

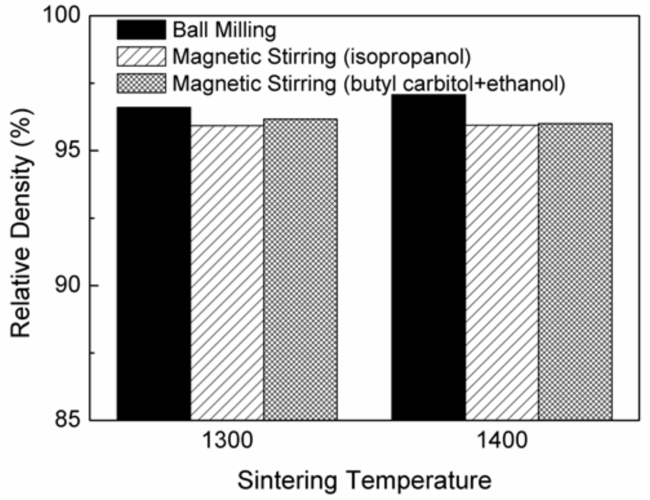

Fig. 8 Relative bulk densities of BYZ (1 wt% ZnO addition) pellets mixed by ball milling and magnetic stirring in isopropanol and BE medias

4. BGC and BSC: Results and Discussion

4.1 Phase of BGC and BSC powders and pellets

The XRD results of the BGC and BSC powders reveal the orthorhombic perovskite $BaCeO_3$ phase (JCPDS: 01-070-1429) (Fig. 9) after calcined at 1050 °C, which is lower than previously reported works (calcining T > 1150 °C for BGC[8,9,12,21] and > 1300 °C for BSC).[10,11,22] After sintering, the XRD analysis of unpolished BGC and BSC pellets shows the presence of additional phases, such as CeO_2 and $BaCO_3$ (Fig. 10). According to Shima and Haile,[21] the presence of CeO_2 phase was associated with the BaO deficiency in BGC samples. Therefore, the appearance of CeO_2 in BGC and BSC is mainly caused by the BaO evaporation, similar to the BYZ results. $BaCO_3$ phase is also commonly observed in doped $BaCeO_3$ due to its phase instability under CO_2-containing atmosphere at

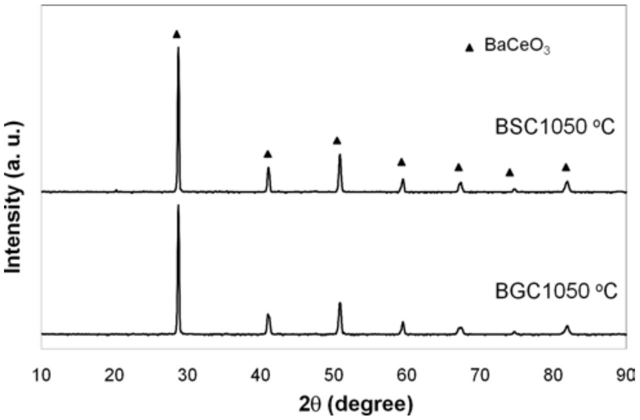

Fig. 9 XRD spectra of BGC and BSC powders after calcination at 1050 °C

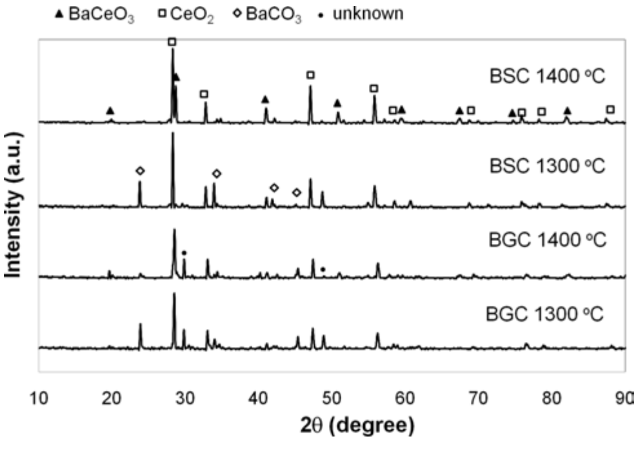

Fig. 10 XRD spectra of unpolished BGC and BSC pellet surfaces after sintered at 1300-1400 °C

temperatures below 1185 °C.[23]

However, in this study, we observe the $BaCO_3$ phase even after sintered at 1300 °C for 10 h. The discrepancy of our results from Scholten et al.[23]'s work may arise from the difference of starting powders, processing conditions and sintering atmosphere. By increasing the sintering temperature to 1400 °C, $BaCO_3$ phase is no longer observed in BSC, and only trace of $BaCO_3$ remains in BGC samples (Fig. 10). After the surface removal, the XRD spectra of BGC and BSC pellets sintered at 1300-1400 °C match only a single $BaCeO_3$ phase (Fig. 11), which in turn confirm that the BaO loss and $BaCO_3$ formation only occurs on the BSC and BGC pellet surfaces.

4.2 Relative bulk density and microstructure of BSC and BGC Pellets

By adding 1 wt% ZnO, the average relative bulk densities of 95.7-96.0% for BGC and 93.3-93.7% for BSC pellets are achieved (Fig. 12). The high relative density of BGC (1 wt% ZnO addition) at the low sintering temperature is obtained primarily due to our nanopowder utilization. The relative bulk density results also reveal that ZnO is an effective sintering aid for BGC, but not for BSC.

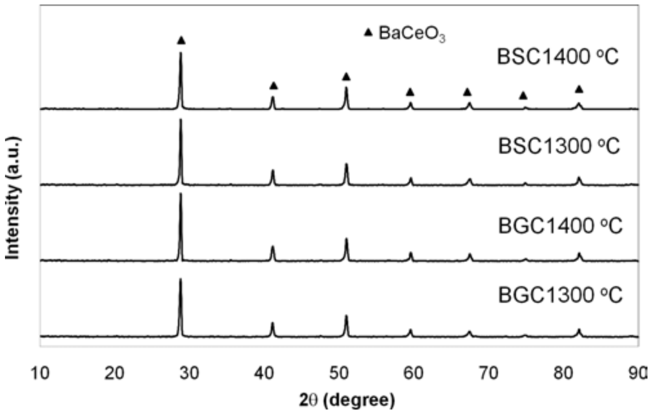

Fig. 11 XRD spectra of polished BGC and BSC pellet surfaces after sintered at 1300-1400 °C

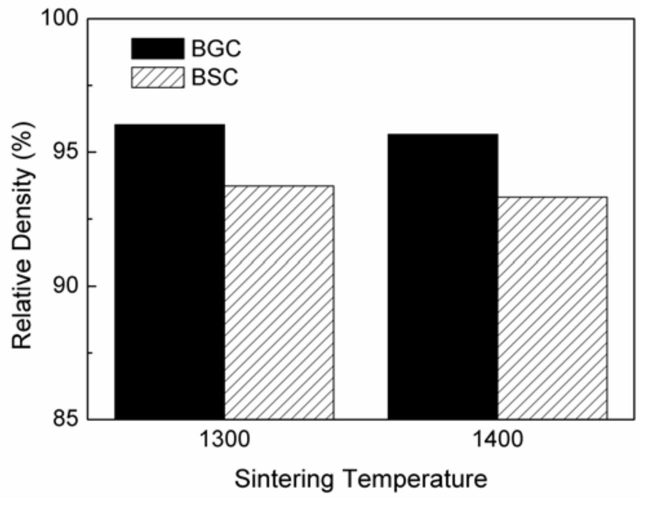

Fig. 12 Relative bulk density of BGC and BSC (1 wt% ZnO addition) pellets after sintered at 1300-1400 °C

The surface microstructures of unpolished and polished BSC and BGC pellets are shown in Fig. 13. Dissimilar to the porous surfaces of unpolished BYZ pellets, the dense surfaces of unpolished BGC and BSC pellets are observed (Fig. 13(a) and 13(c)). The discrepancy of the surface microstructures may be caused by the differences in amount of BaO loss, types of second phases present (CeO_2 and $BaCO_3$ on BSC and BGC surfaces compared to YSZ and Y_2O_3 on BYZ surface) and the bulk densities of those phases. Based on both XRD and SEM results, the surface polishing of BYZ, BSC and BGC pellets must be performed before employing in the PCFC application.

5. Conclusions

By using oxide nanopowders, the calcining temperature of 16 at% BYZ, BGC and BSC could be lowered to 1050 °C. Two mixing methods, ball milling and magnetic stirring (using isopropanol media), utilized for the BYZ preparation provide the similar BYZ powder characteristics. Thus, the magnetic stirring in a suitable solvent can be effectively employed to lower the powder loss in the mixing process.

After the sintering process, due to the BaO evaporation, additional phases were present on the pellet surfaces resulting in the distinction between surface and bulk microstructures. After surface polishing, the dense samples were obtained. With 1 wt% ZnO addition, the relative bulk densities (compared to theoretical densities) of BYZ and BGC were about 96% at the sintering temperature of 1300 °C. Thus, the use of nanopowders together with ZnO as a sintering aid could effectively reduce the sintering temperatures of BYZ and BGC to 1300 °C. Since the relative density of 93% was achieved in BSC samples even after sintered at 1400 °C, other sintering aid should be further studied to increase the bulk density of this material.

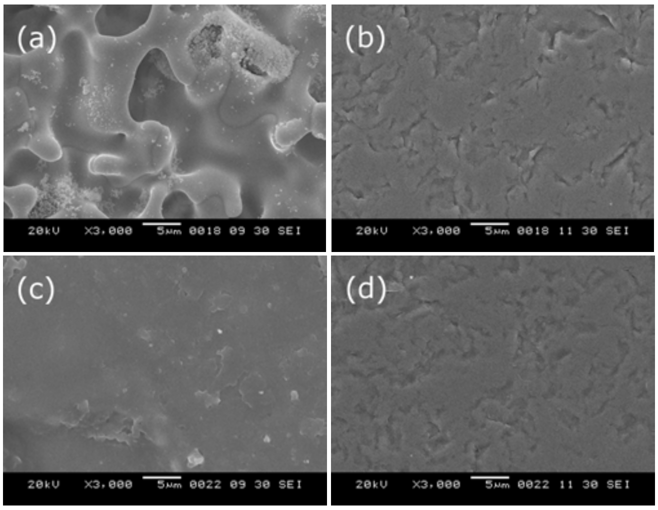

Fig. 13 SEM images of BGC and BSC (1 wt% ZnO addition) surfaces (a) unpolished BGC sintered at 1300 °C (b) polished BGC sintered at 1300 °C (c) unpolished BSC sintered at 1300 °C and (d) polished BSC sintered at 1300 °C

ACKNOWLEDGEMENT

The authors would like to thank Asst. Prof. Dr. Thanakorn Wasanapiarnpong, Asst. Prof. Dr. Wantanee Buggakupta for some essential lab equipments and helpful discussion on the solid state reactions and polishing processes, Adisak Thueploy (The Metallurgy and Materials Science Research Institute, Chulalongkorn University) for the assistance with the cold isostatic pressing, Wirapong Kornpanom for the XRD analysis, and Thanakorn Tepamat for SEM analysis. We also would like to acknowledge the financial support from the Research, Development and Engineering (RD&E) fund through The National Nanotechnology Center (NANOTEC), The National Science and Technology Development Agency (NSTDA), Thailand (Project No. P-11-00984) to Chulalongkorn University.

REFERENCES

1. Kreuer, K. D., “Proton-conducting oxides,” Annu. Rev. Mater. Res., Vol. 33, pp. 333-359, 2003.
2. Kreuer, K. D., Adams, S., Münch, W., Fuchs, A., Klock, U., and Maier, J., “Proton conducting alkaline earth zirconates and titanates for high drain electrochemical applications,” Solid State Ionics, Vol. 145, No. 1-4, pp. 295-306, 2001.
3. Iwahara, H., “Proton conducting ceramics and their applications,” Solid State Ionics, Vol. 86-88, pp. 9-15, 1996.
4. Iwahara, H., Yajima, T., Hibino, T., Ozaki, K., and Suzuki, H., “Protonic conduction in calcium, strontium and barium zirconates,” Solid State Ionics, Vol. 61, No. 1-3, pp. 65-69, 1993.
5. Iguchi, F., Sata, N., Tsurui, T., and Yugami, H., “Microstructures and grain boundary conductivity of $BaZr_{1-x}Y_xO_3$ (x = 0.05, 0.10, 0.15) ceramics,” Solid State Ionics, Vol. 178, No. 7-10, pp. 691-695, 2007.
6. Iguchi, F., Tsurui, T., Sata, N., Nagao, Y., and Yugami, H., “The relationship between chemical composition distributions and specific grain boundary conductivity in Y-doped $BaZrO_3$ proton conductors,” Solid State Ionics, Vol. 180, No. 6-8, pp. 563-568, 2009.
7. Taniguchi, N., Hatoh, K., Niikura, J., Gamo, T., and Iwahara, H., “Proton conductive properties of gadolinium-doped barium cerates at high temperatures,” Solid State Ionics, Vol. 53-56, pp. 998-1003, 1992.
8. Stevenson, D. A., Jiang, N., Buchanan, R. M., and Henn, F. E. G., “Characterization of Gd, Yb and Nd doped barium cerates as proton conductors,” Solid State Ionics, Vol. 62, No. 3-4, pp. 279-285, 1993.
9. Gorbova, E., Maragou, V., Medvedev, D., Demin, A., and Tsiakaras, P., “Influence of sintering additives of transition metals on the properties of gadolinium-doped barium cerate,” Solid State Ionics, Vol. 179, No. 21-26, pp. 887-890, 2008.
10. Gorbova, E., Maragou, V., Medvedev, D., Demin, A., and Tsiakaras, P., “Investigation of the protonic conduction in Sm doped $BaCeO_3$,” J. Power Sources, Vol. 181, No. 2, pp. 207-213, 2008.
11. Iwahara, H., Yajima, T., Hibino, T., and Ushida, H., “Performance of solid oxide fuel cell using proton and oxide ion mixed conductors based on $BaCe_{1-x}Sm_xO_{3-\alpha}$,” J. Electrochem. Soc., Vol. 140, No. 6, pp. 1687-1691, 1993.
12. Venkatasubramanian, A., Gopalan, P., and Prasanna, T. R. S., “Synthesis and characterization of electrolytes based on BaO–CeO_2–$GdO_{1.5}$ system for Intermediate Temperature Solid Oxide Fuel Cells,” Int. J. Hydrogen Energy, Vol. 35, No. 10, pp. 4597-4605, 2010.
13. Tao, S. W. and Irvine, J. T. S., “A Stable, Easily Sintered Proton-Conducting Oxide Electrolyte for Moderate-Temperature Fuel Cells and Electrolyzers,” Adv. Mater., Vol. 18, No. 12, pp. 1581-1584, 2006.
14. Tao, S. and Irvine, J. T. S., “Conductivity studies of dense yttrium-doped $BaZrO_3$ sintered at 1325°C,” J. Solid State Chem., Vol. 180, No. 12, pp. 3493-3503, 2007.
15. Babilo, P. and Haile, S. M., “Enhanced Sintering of Yttrium-Doped Barium Zirconate by Addition of ZnO,” J. Am. Ceram. Soc., Vol. 88, No. 9, pp. 2362-2368, 2005.
16. Peng, C., Melnik, J., Li, J., Luo, J., Sanger, A. R., and Chuang, K. T., “ZnO-doped $BaZr_{0.85}Y_{0.15}O_{3-\delta}$ proton-conducting electrolytes: Characterization and fabrication of thin films,” J. Power Sources, Vol. 190, No. 2, pp. 447-452, 2009.
17. Pornprasertsuk, R., Kosasang, O., Somroop, K., Horprathum, M., Limnonthakul, P., Chindaudom, P., and Jinawath, S., “Proton conductivity of Y-doped $BaZrO_3$: Pellets and thin films,” Solid State Sciences, Vol. 13, No. 7, pp. 1429-1437, 2011.
18. Fabbri, E., Pergolesi, D., Licoccia, S., and Traversa, E., “Does the increase in Y-dopant concentration improve the proton conductivity of $BaZr_{1-x}Y_xO_{3-\delta}$ fuel cell electrolytes?” Solid State Ionics, Vol. 181, No. 21-22, pp. 1043-1051, 2010.
19. Somroop, K., Pornprasertsuk, R., and Jinawath, S., “Fabrication of Y_2O_3-doped $BaZrO_3$ thin films by electrostatic spray deposition,” Thin Solid Films, Vol. 519, No. 19, pp. 6408-6412, 2011.
20. Snijkers, F. M. M., Buekenhoudt, A., Cooymans, J., and Luyten, J. J., “Conductivity and phase composition in $BaZr_{0.9}Y_{0.1}O_{3-\delta}$,” Scripta Materialia, Vol. 50, No. 5, pp. 655-659, 2004.
21. Shima, D. and Haile, S. M., “The influence of cation non-stoichiometry on the properties of undoped and gadolinia-doped barium cerate,” Solid State Ionics, Vol. 97, No. 1-4, pp. 443-455, 1997.
22. Oishi, M., Yashiro, K., Sato, K., Mizusaki, J., Kitamura, N.,

Amezawa, K., Kawada, T., and Uchimoto, Y., “Oxygen nonstoichiometry of the perovskite-type oxides $BaCe_{0.9}M_{0.1}O_{3-\delta}$ (M = Yb, Sm, Tb, and Nd),” Solid State Ionics, Vol. 179, No. 15-16, pp. 529-535, 2008.

23. Scholten, M. J., Schoonman, J., Van Miltenburg, J. C., and Oonk, H. A. J., “Synthesis of strontium and barium cerate and their reaction with carbon dioxide,” Solid State Ionics, Vol. 61, No. 1-3, pp. 83-91, 1993.